Proceedings of the 4th Jagiellonian Symposium on Advances in Particle Physics and Medicine

Safe Proton Radiotherapy for Patients with Metallic Spine Stabilization System

K. Kisielewicz[a,*], E. Góra[a], T. Skóra[a], B. Kiełtyka[b], M. Garbacz[c], M. Rydygier[c], D. Krzempek[c] and R. Kopeć[c]

[a] *The Maria Sklodowska — Curie National Research Institute of Oncology in Kraków, Garncarska 11, 31-115 Kraków*
[b] *University Hospital in Kraków, Jakubowskiego 2, 30-688 Kraków*
[c] *Institute of Nuclear Physics PAN, Cyclotron Centre Bronowice, Radzikowskiego 152, 31-342 Kraków*

Doi: 10.12693/APhysPolA.142.351 *e-mail: kamil.kisielewicz@onkologia.krakow.pl

The brain and the skull base tumors are the most common cases treated in Kraków with proton therapy. Due to the need to deliver a high dose of ionizing radiation (70–74 Gy RBE) and the close presence of critical structures such as the brainstem, optic chiasm, and optic nerves, the use of a proton beam creates better opportunities for dose escalation to the target volume compared to photon radiotherapy. A problem in planning such treatment is the presence of metal stabilizers on the beam path in about 40% of patients, which increases the uncertainty of the planned dose delivery. Acquisition of the computed tomography layers, necessary for treatment planning, was performed with the Siemens Somatom Definition AS apparatus, equipped with the iMAR software, an optimized iterative algorithm for reducing metal artifacts. Then, a dedicated calibration curve for the Varian Eclipse treatment planning system (Hounsfield Units to relative proton stopping power conversion) was prepared. The geometry of the beams is also optimized with respect to the metal element and the critical organs. The presented procedure allowed for the safe proton radiotherapy treatment using a scanning beam in over 50 patients with metallic stabilizers, which was additionally confirmed by Monte Carlo simulations using the FRED tool.

topics: proton radiotherapy, skull base tumors, spine stabilization, metallic implants

1. Introduction

Since the beginning of radiotherapy in Kraków, skull base tumors have been one of the main cases treated here. Tumors of this kind are usually treated with a high dose of ionizing radiation (70–74 Gy RBE) and localized near critical structures. Moreover, in locations such as the base of the skull or the spine, there may be metal stabilizers that may enter the radiation field. It has been already introduced that spinal implants interfere with the dose distributions calculated in the treatment planning system [1].

To prepare a treatment plan using a scanning proton beam, verified experimental data for the treatment planning system, such as beam parameters and calibration curve for the computed tomography (CT) scanner, are needed. For the imaging protocol of the patients with metal components, a dedicated calibration curve is prepared that converts Hounsfield Units (HU) to relative proton stopping power (RPSP). Additionally, patient's target structures, such as planning target volume (PTV) and organs at risk (OARs), contoured by the physician, are necessary for treatment planning and plan evaluation.

The calibration curve is the main source of systematic uncertainty in the planning of proton radiotherapy as it determines the beam range calculated by the treatment planning system (TPS) at a given proton energy [2]. In patients who have metal element, CT image artifacts appear, giving false information about the density of the medium. Instead of the HU numbers characteristic of soft tissue or bone tissue, their significant reduction is visible — even to the value corresponding to the air.

There are three main sources of artifacts on a CT image with metal elements:

1. Beam hardening — where low-energy photons are much more absorbed by the metal element. High-energy photons passing through metal do not provide adequate image quality, especially for soft tissues.

2. Undersampling — the area with a large difference in densities (metal and surrounding tissue) is not sampled sufficiently.
3. "Photon Starvation" — where a small number of photons is registered by the CT system, which increases the statistical uncertainty.

The above-mentioned factors causing the formation of artifacts on CT images with metal stabilizers significantly increase the range uncertainty, empirically determined at 3.5% for the regular medium [3].

2. Material and methods

In order to safely plan the treatment for patients with metal stabilizers, it is necessary to eliminate the artifacts derived from metal, visible on the CT image, and to obtain complete information about the HU numbers for the metal material. Artifacts on the CT image can be corrected manually, however, it is time-consuming and not very accurate. Dedicated algorithms, cooperating with a computed tomography system, can be also used. Only CT layers with eliminated artifacts can be used to prepare an appropriate treatment plan.

2.1. Metal artifact reduction

At the National Institute of Oncology in Kraków, two software solutions are available to reduce metal artifacts. The first is MARS (Metal Artifacts Reduction Software) — installed on the GE Discovery 750 HD CT scanner. It uses a dual-energy solution (differences in cross-sections for photon interactions as a function of energy). Image reconstruction is carried out using filtered back projection (FBP) method. The second one, i.e., Siemens Somatom Definition AS, uses a single energy Iterative Metal Artifacts Reduction (iMAR) software, based on iterative reconstruction with respect to a given/expected preset. To assess which of the available tools is better for eliminating artifacts, a special phantom was built containing (see Fig. 1) a titanium spine stabilizer embedded in gelatin.

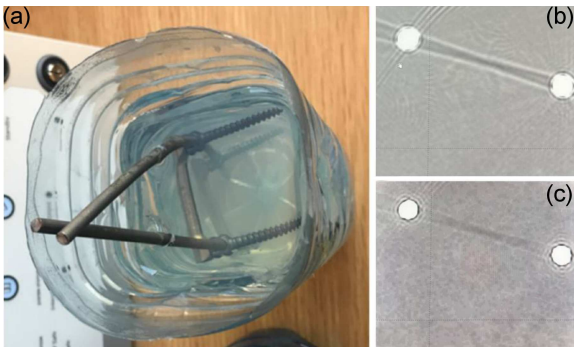

Fig. 1. (a) Spine stabilization system in the phantom; (b) phantom's image reconstructed by MARS; (c) phantom's image reconstructed by iMAR.

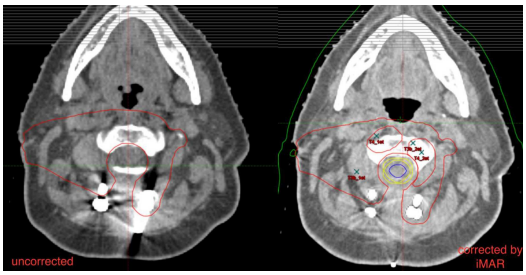

Fig. 2. Metal artifacts correction with Siemens iMAR algorithm.

The stabilization system was made from Ti 6AL4V alloy (6% of aluminum and 4% of vanadium added) as a routinely used clinical spine stabilization system.

The prepared phantom with Ti stabilizers was scanned in a bigger water phantom on each tomograph, using both methods of reduction metal artifacts. The placement of the gelatin phantom inside the water phantom is closer to the clinical condition in terms of the field of the view and the attenuation of the scanner radiation. A visual assessment of the phantom images was carried out. The iMAR reconstructed images have less artifacts. Based on the above, a Siemens CT with an iterative algorithm reducing artifacts was used for further work. The example of the CT scan corrected with iMAR algorithms is shown in Fig. 2.

Acquisition of CT layers was performed with the Siemens Somatom Definition AS apparatus using the iMAR iterative algorithm optimized for the purpose of reducing metal artifacts. Then, a protocol dedicated for iMAR calibration curve was prepared. For each patient having a stabilizer, computed tomography was additionally reconstructed in the extended HU scale to transfer information necessary for treatment planning algorithm like implant density [4]. Then, high-density structures from the extended HU scale were copied to planning CT. Acquired CT values of metal elements were assigned on CT prepared for treatment planning.

When iMAR did not correct the image as expected, artifacts were manually overwritten using the HU values, from tissue of a close density to the expected one.

Planning CT used a dedicated iMAR calibration curve up to the 9074 HU as there was no denser insert available in the calibration phantom. Materials with the HU numbers greater than the last point of the calibration curve were overwritten with 9074 HU after contouring.

2.2. Preparing beam geometry

In tumors of the base of the skull, especially chordomas and chondrosarcomas, the PTV area surrounds the spinal canal on the anterior and lateral sides. For patients after implantation, the appropriate beam geometry should be selected in

addition to the artifact reduction method presented in the paragraph above. The direction of the beams should be selected so that the metal element is not in the path of the beam, which is very difficult to achieve. In clinical practice, the beam should not pass proximally through the metal element in relation to the spinal canal and other critical organs at risk, if present.

Treatment plans were also based on individually defined structures, the so-called "target per field" (TPF), i.e., volumes to be irradiated from a given therapeutic beam. The purpose of this method is to avoid fragmented artifact areas being reconstructed in an unacceptable way. The geometry of the beams and TPFs have also been optimized with respect to the metal component and critical organs.

2.3. Range uncertainty

Due to the multiple sources of proton beam range uncertainties (including both biological [5] and physical uncertainties [6]), it is possible to calculate an additional margin for PTV reducing the influence of the beam range uncertainty on the target coverage. Range uncertainties were calculated for the clinical target volume (CTV) structure separately for each of the field according to the formulae:

- Proximal margin (PM)

$$\mathrm{PM} = \big(\mathrm{NR} - \mathrm{SOBP}\big) \times 3.5\% + 0.1\,\mathrm{cm}, \tag{1}$$

- Distal margin (DM)

$$\mathrm{DM} = \mathrm{NR} \times 3.5\% + 0.1\,\mathrm{cm}, \tag{2}$$

where NR — nominal range (energy-dependent) given in cm, SOBP — spread out Bragg peak width of the target, given in cm.

An additional 0.1 cm margin was added to account for the uncertainty of patient movement to ensure PTV coverage. A treatment plan was then prepared for the defined beam geometry in the Eclipse v. 16.1 treatment planning system (Varian Medical Systems) in inverse planning technique using Non-Linear Universal Proton Optimizer (NUPO), which allows to reduce plan uncertainty by robust optimization.

2.4. Analysis

For the clinically accepted plan, assuming the same conditions (regarding CT scan, structure set, and beam geometry), the dose distribution was calculated using the Monte Carlo tool FRED (Fast paRticle thErapy Dose evaluator). The result — as dose-to-medium — was experimentally and clinically validated in Kraków [7].

For both calculation methods (PTS, Fred), the same data (especially dedicated to iMAR) was used to prepare the CT calibration curve for the relative proton stopping power (RPSP). It can cause systematic variation for the calculated doses, so the precise preparing of such relationship is crucial to minimize systematic error. Several methods of CT calibration can be found in the literature. The most common is the one proposed by Schneider et al. [8], the so-called stechiometric method, which allows to minimize the uncertainties of the calculation ranges to the level of 3.5% of the beam range [9]. The method was used to prepare the CT calibration curves in this case.

Finally, a dose distribution comparison was made in Sun Nuclear SNC Patient software using the gamma method for the parameters: dose difference DD = 3%, distance to agreement DTA = 2 mm, threshold of 60%. Doses for PTVs and OARs were evaluated and compared in Eclipse TPS.

To date, treatment has been finished for more than 50 patients with cervical/occipital stabilizer, without any signs of complications in follow-up. Monte Carlo calculation was performed for 10 patients using the Fred tool. Due to the anatomical location of PTVs, the spinal cord with extra 3 mm margin, was a critical organ analyzed for all 10 patients (maximum point dose). In addition, for three of them — brainstem maximum doses were also analyzed.

3. Results

Due to the different doses assigned to the treatment volumes in the treatment plans, the differences in doses received by critical organs and target structures as calculated by TPS Eclipse and MC FRED were relatively assessed.

An example of a dose distribution in a patient with chordoma is presented in Fig. 3. The maximum doses expressed in Gy RBE for the spinal cord + 3 mm were compared. The differences between the Eclipse and MC Fred calculations ranged from 0.65 to 6.95% with an average value of 2.86% and a standard deviation of 2%. Doses for brainstem were also compared in a similar way. The differences between the Eclipse and MC Fred calculations ranged from 0.11 to 3.97%, respectively, with an average value of 1.61% and a standard deviation of 2% (see Table I).

Target structures were also analyzed, i.e., GTV (gross tumor volume), CTV (clinical target volume), PTV (planning target volume), for the parameters: near minimum dose — $D_{98\%}$, mean dose — D_{mean}, near maximum dose — $D_{2\%}$. The results are shown in Table II.

Additionally, a comparison of the dose distributions calculated by MC Fred and TPS Eclipse for the five transverse layers for each patient

TABLE I

Maximum doses D_{max} for organs at risk (OARs).

OAR	D_{max} Eclipse vs D_{max} Fred [%]
Spinal cord + 3 mm	2.86 ± 1.99
Brainstem	1.61 ± 2.07

TABLE II

Reported doses for target structures.

Target structure	$D_{98\%}$ Eclipse vs $D_{98\%}$ Fred [%]	D_{mean} Eclipse vs D_{mean} Fred [%]	$D_{2\%}$ Eclipse vs $D_{2\%}$ Fred [%]
GTV	3.32 ± 2.09	1.27 ± 0.79	1.62 ± 1.17
CTV	6.87 ± 2.42	1.80 ± 1.21	1.47 ± 0.82
PTV	7.89 ± 3.97	1.36 ± 1.10	1.86 ± 0.9

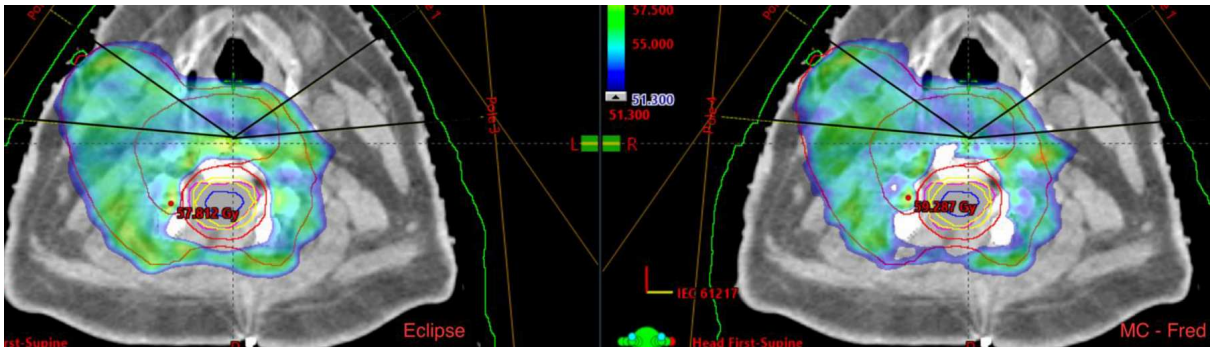

Fig. 3. Dose distribution for TPS Eclipse vs MC Fred tool. Black lines correspond to the beam's direction.

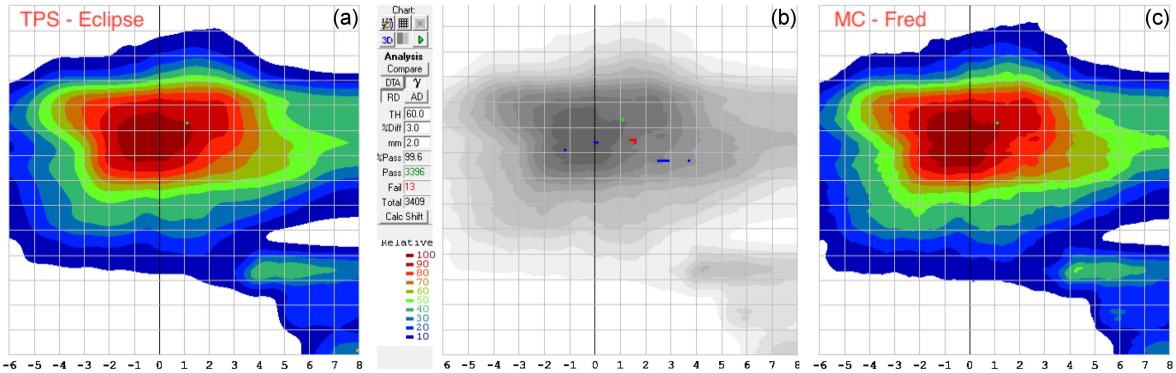

Fig. 4. Fred vs Eclipse doses — gamma evaluation for 3% and 3 mm. In panel (a), TPS dose distribution is presented. Panel (c) presents MC generated dose distribution. Panel (b) corresponds to gamma difference.

was performed using the gamma method. A clinically acceptable agreement between layers is when gamma ≤ 1 is met for more than 90% of the pixels.

An example of the analyzed layer is presented in Fig. 4. The average percent of pixels meeting the gamma criteria was 95.7 (values from 85.8 to 100) with a standard deviation of 3.9. Out of the 50 dose layers analyzed, only 2 did not meet defined clinical requirements.

4. Conclusions

The presented procedure allowed for safe proton radiotherapy using proton-pencil beam scanning in over 50 patients with metallic stabilizers, which was additionally confirmed by Monte Carlo simulations with the FRED tool. The dose for the selected organs at risk (spinal cord and brainstem) is the same in the MC calculation as in TPS. For OARs, the maximum difference between the Eclipse dose and Fred calculation is 7%, which is a clinically satisfactory result. A good agreement of the TPS dose distribution with the MC dose distribution was obtained, as confirmed by gamma analysis. Only 4% of dose layers did not meet clinical requirements. Therefore, it is possible to reduce the uncertainty of the treatment plan by reducing metallic artifacts and selecting the appropriate beam geometry in relation to critical organs and metal elements. It will allow safe proton radiotherapy with a stabilizer in this critical area of the base of skull tumors.

As one of the few proton radiotherapy centers in the world, we safely treat patients with spine and skull base stabilizers using proton-pencil beam scanning. This is a significant complement to the development of radiotherapy in Poland [10].

References

[1] Y. Jia, L. Zhao, C.-W. Cheng, M.W. McDonald, I.J. Das, *J. Appl. Clinic. Med. Phys.* **16**, 333 (2015).

[2] J. Schuemann, S. Dowdell, C. Grassberger, C.H. Min, H. Paganetti, *Phys. Med. Biol.* **59**, 4007 (2014).

[3] M. Goitein, *Radiation Oncology: A Physicist's-Eye View*, Springer, New York 2008.

[4] J.P. Mullins, M.P. Grams, M.G. Herman, D.H. Brinkmann, J.A. Antolak, *J. Appl. Clinic. Med. Phys.* **17**, 179 (2016).

[5] M. Garbacz, J. Gajewski, M. Durante et al., *Rad. Oncol.* **17**, 50 (2022).

[6] E.J. Tryggestad, W. Liu, M.D. Pepin, C.L. Hallemeier, T.T. Sio, *J. Gastrointest. Oncol.* **11**, 212 (2020).

[7] J. Gajewski, M. Garbacz, C.-W. Chang et al., *Front. Phys.* **8**, 1 (2021).

[8] U. Schneider, E. Pedroni, A. Lomax, *Phys. Med. Biol.* **41**, 111 (1996).

[9] J. Schuemann, S. Dowdell, C. Grassberger, C.H. Min, H. Paganetti, *Phys. Med. Biol.* **59**, 4007 (2014).

[10] R.W. Gryglewski, *Bio-Algorithms Med-Syst.* **17**, 227 (2021).